Int. J. Nonlinear Anal. Appl. 12 (2021) No. 1, 365-383
ISSN: 2008-6822 (electronic)
http://dx.doi.org/10.22075/ijnaa.2021.4810

# Stable numerical solution of an inverse coefficient problem for a time fractional reaction-diffusion equation

Afshin Babaei[a,*], Seddigheh Banihashemi[a], Javad Damirchi[b]

[a]Department of Applied Mathematics, University of Mazandaran, P.O. Box: 47416-95447, Babolsar, Iran
[b]Department of Mathematics, Faculty of Mathematics, Statistics and Computer Science, Semnan University, Semnan, Iran

(Communicated by Madjid Eshaghi Gordji)

**Abstract**

In this paper, an inverse problem of determining an unknown reaction coefficient in a one-dimensional time-fractional reaction-diffusion equation is considered. This inverse problem is generally ill-posed. For this reason, the mollification regularization technique with the generalized cross-validation criteria will be employed to find an equivalent stable problem. Afterward, a finite difference marching scheme is introduced to solve this regularized problem. The stability and convergence of the numerical solution are investigated. In the end, some numerical examples are presented to verify the ability and effectiveness of the proposed algorithm.

*Keywords:* Inverse problem, Time fractional reaction-diffusion equation, Caputo's fractional derivative, Mollification, Marching scheme.
*2010 MSC:* Primary 65M32; Secondary 35R11, 35R30.

## 1. Introduction

In recent decades, the fractional order derivative and integral operators have found many applications in science disciplines [5, 21, 24, 37, 39]. The fractional order derivatives are nonlocal and have memory effects, namely, in a fractional system, the next state depends on its current and all previous states. Thus, fractional differential and integral equations have been used widely to model a range of phenomena in different fields of science, such as physics, chemistry, biology and engineering [5, 10, 12,

*Corresponding author
*Email addresses:* babaei@umz.ac.ir (Afshin Babaei), s.banihashemi@stu.umz.com (Seddigheh Banihashemi), damirchi@profs.semnan.ac.ir (Javad Damirchi)

*Received:* 11 October 2017 *Revised:* 25 June 2020

17, 21, 23, 24, 26, 37, 39]. Fractional diffusion equations are one of the most important equations to make mathematical formulations of these real applications. References [10, 17, 26, 39] and the other references cited therein reveal the fundamental properties of time-fractional diffusion equations.

Many phenomena in science and engineering have been modeled in the form of inverse problems [2, 3, 4, 6, 25]. These types of problems are suitable for dealing with the models containing some unknown input information. Optical tomography [2], scattering of waves [9], heat conduction [6], machine learning [25], water and air pollution intensity [22] are examples of these applications. Based on the recent developments in the fractional order differential equations, researchers have used these new concepts to generalize some previously presented models. Thus, some useful papers have been published about the fractional order inverse problems. The studies of these scientists have led to some interesting computational ways for solving inverse problems of fractional types [8, 14, 20, 29, 30, 32, 34, 35, 36, 38]. In these papers, various numerical schemes have been proposed to solve inverse problems of time fractional type, such as finite difference methods [20, 30], spectral regularization method [38], quasi-Newton method [14], the quasi-boundary value method [34], boundary element method [35], the method of fundamental solutions [8, 36], the homotopy regularization algorithm based on the error functional [29] and modulating functions method [1]. Fractional order inverse problems are generally ill-posed. Thus, using appropriate regularization methods are necessary to find a stable numerical solution for these problems. In this article, the time-fractional order reaction-diffusion equation

$$\mathrm{D}_{0,t}^{\alpha} u(x,t) = u_{xx}(x,t) - q(x)u(x,t) + f(x,t), \quad (x,t) \in \Omega \times \mathcal{I}, \tag{1.1}$$

with the initial and the boundary conditions

$$u(x,0) = u_0(x), \qquad x \in \Omega, \tag{1.2}$$
$$u_x(0,t) - \sigma u(0,t) = 0, \qquad t \in \mathcal{I}, \tag{1.3}$$
$$u_x(1,t) + \gamma u(1,t) = 0, \qquad t \in \mathcal{I}, \tag{1.4}$$

is considered. $f(x,t)$ shows the source term, $q(x)$ is unknown reaction coefficient and $u_0(x)$ is the given initial function. Also, $\Omega := (0,1)$, $\mathcal{I} := (0,1)$ and the known constants $\sigma, \gamma \in \mathbb{R}$ in boundary conditions (1.3) and (1.4) are correspond to the insulation parameters at both ends [32]. Also, $\mathrm{D}_{0,t}^{\alpha} u$ means Caputo's fractional derivative of order $\alpha \in (0,1)$ defined as [21]:

$$\mathrm{D}_{0,t}^{\alpha} u(x,t) = \frac{1}{\Gamma(1-\alpha)} \int_0^t (t-s)^{-\alpha} u_s(x,s) ds, \qquad t \in \mathcal{I},$$

where $\Gamma(.)$ is the Gamma function. Eq. (1.1) comes from numerous practical applications. The anomalous diffusion equation is one of these cases which is characterized by the property that its variance behaves like a non-integer power of time [7, 16, 17]. The anomalous non-Markovian diffusion process is often observed in materials with memory, e.g., viscoelastic materials, and heterogeneous media, such as soil, heterogeneous aquifer, and underground fluid flow [13]. Hence, fractional derivatives are useful tools for describing sub-diffusion phenomena, which are characterized by a heavy-tailed waiting time distribution in diverging temporal moments and non-Markovian dynamics. A fractional reaction-diffusion equation can be derived from a continuous time random walk model with temporal memory and sources [11] or a continuous time random walk model when the transport is dispersive [27]. In the medical sciences, the temperature and the blood perfusion coefficient $q(x)$ are related through the Pennes bio-heat conduction equation given by the equation (1.1). The accurate estimations of temperature and blood perfusion rate through a certain region of tissue is

an important task during a surgical operation [31]. Considering this problem as an inverse problem, help researchers to determine both the temperature u and the perfusion coefficient $q(x)$. Also, according to the properties of nonlocality [21, 24], fractional derivatives are useful tools to model the multidirectional nonlocal flow through the living tissue. The Robin boundary conditions (1.3) and (1.4) occur in many physical phenomena. In heat conduction process, under the assumption that the heat fluxes across the boundaries of the problem are as functions of temperature, we will have nonlinear boundary conditions [13].

To our knowledge, there are a few works concerned with the inverse problems related to the time-fractional reaction-diffusion equations. An iteration scheme for the numerical reconstruction of the nonlinear source term in a reaction-diffusion problem was discussed in [15]. In [32, 33] the unique solvability of the inverse problem to recover the unknown coefficients of a multidimensional fractional reaction-diffusion equation under the Dirichlet and the Neumann boundary conditions was proved. In [28] a multi-parameter regularization $L^2 + BV$ method was presented to solve a reaction coefficient inverse problem for time fractional reaction-diffusion equation with Neumann boundary data in two dimensional spaces.

To determine the reaction coefficient $q(x)$ in the inverse problem (1.1)-(1.4), we need an additional condition. Here, the condition

$$u(1,t) = \phi(t), \qquad t \in \mathcal{I}, \tag{1.5}$$

is used. The existence and uniqueness of the solution to this problem have been investigated in [32]. No numerical method has been given by the authors in the literature to solve the problem (1.1)-(1.5). Furthermore, in addition to the ill-posedness of the inverse coefficient problem, the process of numerical fractional differentiation is well known to be an ill-posed problem [19], because the fractional derivative is defined by a nonlocal weak singular integration. So, a small error in measurement data can induce a large error in the approximate derivative. Thus, proposing a reliable algorithm to find the numerical solution of this type of fractional problem may be useful for researchers. In practice, the input functions of the problem are not exact, but some perturbed versions of them are in hand. Thus, we first stabilize this problem by a mollification regularization method [18]. Afterwards, a numerical scheme based on the space marching method is introduced to approximate the solution of (1.1) and the unknown coefficient $q(x)$.

This paper consists four sections. In Section 2, a regularization technique is proposed to stabilize the inverse problem (1.1)-(1.5). In Section 3, the marching algorithm for the numerical solution of the mollified problem is described and the stability and convergence of the numerical conclusion are analysed. Finally, in Section 4, some numerical examples are investigated.

## 2. Ill-posedness and regularization of the inverse problem

The time-fractional inverse problem with unknown reaction coefficient is generally a type of ill-posed problems, because a small error in the input data can cause a large error in the solution of the problem [13, 20]. In practice, the input function $\phi(t)$ in (1.5) is not exact, but some perturbed approximations of that is in hand. Thus, this perturbed function can affect on the solution of the problem. For more illustration, we study a numerical test problem. Consider the problem (1.1)-(1.5) with $\sigma = 1$, $\gamma = -1$, $u_0(x) = e^x$ and

$$f(x,t) = \frac{e^x t^{1-\alpha}}{\Gamma(2-\alpha)} + e^x(1+t)(E_\alpha(x^\alpha)(1-x) - 1),$$

where $E_\alpha(.)$ is the Mittag-Leffler function [24]. Suppose we have two sample input functions $\phi_1(t) = e^1(1+t)$ and $\phi_2(t) = \phi_1(t) + 0.1$. Now the reaction coefficients $q_1(x)$ and $q_2(x)$ dependent on $\phi_1(t)$,

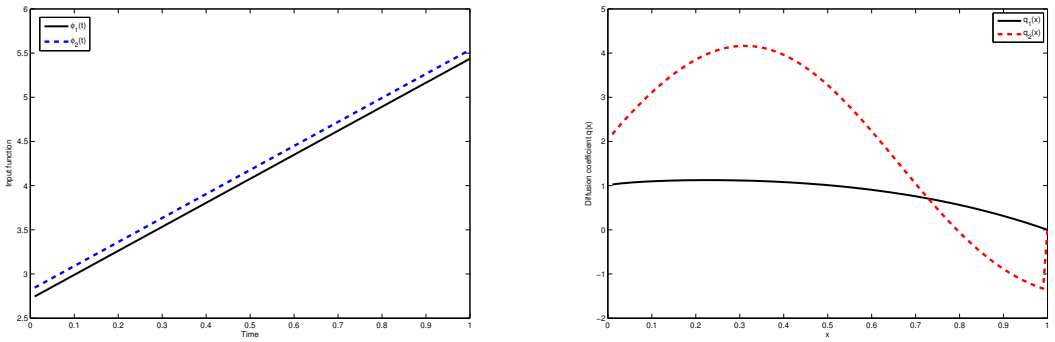

Figure 1: The two estimated reaction coefficients $q_1(t)$ and $q_2(t)$ (Right) correspond to the two close input functions $\phi_1(t)$ and $\phi_2(t)$ (Left).

and $\phi_2(t)$, are calculated by using the proposed algorithm in Section 3. Figure 1 indicates the input functions $\phi_i(t),\ i = 1, 2$, and the approximated reaction coefficients $q_i(x),\ i = 1, 2$. Although these input conditions are very close, but the calculated reaction coefficients dependent on them are far more than we expected. This example shows ill-posedness of the inverse problem. Thus, using appropriate regularization methods is necessary to find a stable numerical solution of the problem.

In this work, we will use the mollification approach to stable the perturbed problem. For this purpose, first we review some basic definitions in the mollification method. Let $\mathrm{C}^0(\mathcal{I})$ denote the set of continuous real functions over the unit interval $\mathcal{I}$ with norm

$$\|g\|_{\infty,\mathcal{I}} = \max_{t\in\mathcal{I}} |g(t)|.$$

Let $\delta > 0$, $p > 0$, and

$$\mathcal{A}_p = \Big( \int_{-p}^{p} exp(-s^2)ds \Big)^{-1}.$$

For $g(t) \in L^1(\mathcal{I})$ and $t \in \mathcal{I}_\delta = [p\delta, 1 - p\delta]$, the $\delta$-mollification of $g(t)$ is defined as follows:

$$\mathcal{J}_\delta g(t) = (\rho_\delta * g)(t) = \int_{t-p\delta}^{t+p\delta} \rho_\delta(t - s)g(s)ds,$$

where

$$\rho_{\delta,p}(t) = \begin{cases} \mathcal{A}_p\delta^{-1}exp(-\frac{t^2}{s^2}), & |t| \le p\delta, \\ 0, & |t| > p\delta. \end{cases}$$

Notice that, the Gaussian kernel $\rho_{\delta,p}$ is a non-negative $\mathrm{C}^\infty(-p\delta, p\delta)$ function satisfying $\int_{-p\delta}^{p\delta} \rho_{\delta,p}(t)dt = 1$. The radius of mollification $\delta$ is determined automatically by the Generalized Cross Validation (GCV) criteria [18]. In order to define the mollification of a discrete function, let $\bar{\mathcal{I}} = \{t_j : j \in \mathbb{Z}\} \subset \mathcal{I}$ and

$$\Delta t = \sup\{(t_{j+1} - t_j) :\ j \in \mathbb{Z},\ t_{j+1} - t_j > d > 0\},$$

where $\mathbb{Z}$ is a set of integers, and d is a positive constant. Let $\mathrm{G} = \{g(t_j) = g_j : j \in \mathbb{Z}\}$ be a discrete function defined on $\bar{\mathcal{I}}$. We set

$$s_j = \frac{1}{2}(t_j + t_{j+1}) \ , \quad j \in \mathbb{Z}.$$

The discrete $\delta$-mollification of G is defined as follows:

$$\mathcal{J}_\delta \mathrm{G}(t) = \sum_{j=-\infty}^{\infty} \Big( \int_{s_{j-1}}^{s_j} \rho_\delta(t-s)ds \Big) g_j.$$

Notice that

$$\sum_{j=-\infty}^{\infty} \Big( \int_{s_{j-1}}^{s_j} \rho_\delta(t-s)ds \Big) = \int_{-p\delta}^{p\delta} \rho_\delta(s)ds = 1.$$

Now, let in the problem (1.1)-(1.5), $\phi(t)$ and $u_0(x)$ are only known approximately as $\phi^\varepsilon$ and $u_0^\varepsilon$, such that the infinity norm of the difference between every of these functions and their corresponding approximations are less than a known value $\varepsilon$. Suppose $\upsilon = \mathcal{J}_\delta u$ is the mollified version of $u$. So, the regularized problem is formulated as follows

$$\begin{aligned}
\mathrm{D}_{0,t}^\alpha \upsilon(x,t) &= \upsilon_{xx}(x,t) - q(x)\upsilon(x,t) + f(x,t), \qquad (x,t) \in \Omega \times \mathcal{I}, && (2.1)\\
\upsilon(1,t) &= \mathcal{J}_\delta \phi^\varepsilon(t), \qquad t \in \mathcal{I}, && (2.2)\\
\upsilon(x,0) &= \mathcal{J}_{\delta'} u_0^\varepsilon(x), \qquad x \in \Omega, && (2.3)
\end{aligned}$$

where $\delta$ and $\delta'$ are the radii of mollification, and will be chosen using the GCV criteria.

Before we introduce the numerical procedure for the above stabilized problem, we notice that the process of numerical fractional differentiation is well known to be ill-posed [19]. Hence, we will use the mollified fractional derivative on our calculations.

Suppose $g^\varepsilon(t)$ is a perturbed version of the exact function $g(t)$. To approximate $\mathcal{J}_\delta(\mathrm{D}_{0,t}^\alpha g^\varepsilon)$ on a uniform partition $\bar{\mathcal{I}}$ of the unit interval, we follow the mollification technique proposed in [19].

Let $\mathfrak{D}_+$ be forward finite difference operator and $\mathfrak{D}_0$ be the centered finite difference operator. The discrete computed fractional order derivative, denoted $(\mathrm{D}_{0,t}^\alpha \mathrm{G}^\varepsilon)_\delta$, in the grid points, will be as

$$\begin{aligned}
\Big(\mathrm{D}_{0,t}^\alpha \mathrm{G}^\varepsilon\Big)_\delta(t_1) &= \mathfrak{D}_+(\mathcal{J}_\delta \mathrm{G}^\varepsilon)(t_1)\omega_1, && (2.4)\\
\Big(\mathrm{D}_{0,t}^\alpha \mathrm{G}^\varepsilon\Big)_\delta(t_2) &= \mathfrak{D}_+(\mathcal{J}_\delta \mathrm{G}^\varepsilon)(t_1)\omega_2 + \mathfrak{D}_+(\mathcal{J}_\delta \mathrm{G}^\varepsilon)(t_2)\omega_1, && (2.5)
\end{aligned}$$

and

$$\Big(\mathrm{D}_{0,t}^\alpha \mathrm{G}^\varepsilon\Big)_\delta(t_j) = \mathfrak{D}_+(\mathcal{J}_\delta \mathrm{G}^\varepsilon)(t_1)\omega_j + \sum_{i=2}^{j-1} \mathfrak{D}_0(\mathcal{J}_\delta \mathrm{G}^\varepsilon)(t_i)\omega_{j-i+1} + \mathfrak{D}_+(\mathcal{J}_\delta \mathrm{G}^\varepsilon)(t_j)\omega_1, \tag{2.6}$$

where $j = 3, 4, ..., n$ and the quadrature weights $\omega_j = \omega_j(\alpha, t_j)$ are integrated exactly with values

$$\begin{aligned}
\omega_1 &= \frac{(\Delta t)^{1-\alpha}}{\Gamma(2-\alpha)\ 2^{1-\alpha}},\\
\omega_i &= \frac{(\Delta t)^{1-\alpha}}{\Gamma(2-\alpha)\ 2^{1-\alpha}} \Big[ (2i+1)^{1-\alpha} - (2i-1)^{1-\alpha} \Big], \quad i = 2, 3, ..., j-1,
\end{aligned}$$

and

$$\omega_j = \frac{1}{\Gamma(2-\alpha)} \Big[ j\Delta t - \Big[ \Big( j - \frac{1}{2} \Big) \Delta t \Big]^{1-\alpha} \Big].$$

## 3. Numerical procedure

In this section, a numerical algorithm will be presented to find the solution of (2.1)-(2.3). Let $M$ and $N$ are positive integers. Consider a uniform grid in the unit interval $[0,1]\times[0,1]$ as

$$\{(x_i = ih, t_n = nk)\ ,\quad i = 0,1,...,M;\quad n = 0,1,...,N\},$$

in which $Mh = 1$ and $Nk = 1$. Let the value of $\upsilon(x,t)$ at $(x_i,t_n)$ is indicated by $\mathsf{R}_i^n$. In addition, suppose

$$\mathsf{W}_i^n = \upsilon_x(ih,nk),\quad \mathsf{Q}_i^n = D_t^{(\alpha)}\upsilon(ih,nk),\quad \mathsf{q}_i = q(ih),\quad \mathsf{F}_i^n = f(ih,nk).$$

Notice that for $n\in\{0,...,N\}$

$$\mathsf{R}_M^n = \mathcal{J}_\delta\phi^\varepsilon(nk),\qquad \mathsf{Q}_M^n = \mathrm{D}_{0,t}^\alpha\mathcal{J}_\delta\phi^\varepsilon(nk).$$

From (1.4), we obtain

$$\mathsf{W}_M^n = -\gamma\mathcal{J}_\delta\phi^\varepsilon(nk),\quad n\in\{0,...,N\},$$

and for $i\in\{0,...,M\}$

$$\mathsf{R}_i^0 = \mathcal{J}_{\delta'}u_0^\varepsilon(ih),\quad \mathsf{W}_i^0 = \mathfrak{D}_0(\mathcal{J}_{\delta'}u_0^\varepsilon(ih)),\quad \mathsf{T}_i = \mathfrak{D}^2(\mathcal{J}_{\delta'}u_0^\varepsilon(ih)),$$

where $\mathfrak{D}^2 := \mathfrak{D}_+\mathfrak{D}_-$ is second-order finite differences operator. From (2.1), we obtain

$$\mathsf{q}_M = \frac{1}{\mathsf{R}_M^0}(\mathsf{T}_M - \mathsf{Q}_M^0 + \mathsf{F}_M^0).$$

Now we approximate the partial differential equation of fractional order in system (2.1)-(2.3) by the finite difference schemes

$$\mathsf{R}_{i-1}^n = \mathsf{R}_i^n - h\mathsf{W}_i^n, \tag{3.1}$$
$$\mathsf{W}_{i-1}^n = \mathsf{W}_i^n - h(\mathsf{Q}_i^n + \mathsf{q}_i\mathsf{R}_i^n - \mathsf{F}_i^n), \tag{3.2}$$
$$\mathsf{Q}_{i-1}^n = \mathrm{D}_{0,t}^\alpha(\mathcal{J}_{\delta_{i-1}}\mathsf{R}_{i-1}^n), \tag{3.3}$$
$$\mathsf{q}_{i-1} = \frac{1}{\mathsf{R}_{i-1}^0}(\mathsf{T}_{i-1} - \mathsf{Q}_{i-1}^0 + \mathsf{F}_{i-1}^0), \tag{3.4}$$

where $i = M, M-1, ..., 1$ and $n = 0,1,...,N$. To approximate $\mathrm{D}_{0,t}^\alpha(\mathcal{J}_{\delta_i}\mathsf{R}_i^n)$, the quadrature formula (2.4)-(2.6) will be used.

## 4. Stability and convergence analysis

In this section, the stability and convergence of the numerical conclusion are analysed.

**Theorem 4.1.** *(Stability of the algorithm) Suppose* $|\mathsf{R}_i|$, $|\mathsf{W}_i|$, $|\mathsf{Q}_i|$ *are maximum values of* $|\mathsf{R}_i^n|$, $|\mathsf{W}_i^n|$, $|\mathsf{Q}_i^n|$, *where* $n = 0,1,...,N$. *For the marching scheme, there exist two constants* $\theta_1$ *and* $\theta_2$, *such that*

$$\max\{|\mathsf{R}_0|,|\mathsf{W}_0|,|\mathsf{Q}_0|,|\mathsf{q}_0|\} \le \theta_1\max\{|\mathsf{R}_M|,|\mathsf{W}_M|,|\mathsf{Q}_M|,|\mathsf{q}_M|\} + \theta_2.$$

**Proof .** Let $M_f = \max_{x,t\in[0,1]}\{|f(x,t)|\}$. By using (3.1) and (3.2), we have

$$|\mathsf{R}_{i-1}^n| \le (1+h)\max\{|\mathsf{R}_i^n|, |\mathsf{W}_i^n|\}, \tag{4.1}$$

$$|\mathsf{W}_{i-1}^n| \le (1+h)\max\{|\mathsf{R}_i^n|, |\mathsf{W}_i^n|, |\mathsf{Q}_i^n|, |\mathsf{q}_i|\} + hM_f. \tag{4.2}$$

Let $\bar{\delta} = \min_i\{\delta_i\}$. From (3.3) and Eq.(30) in [4], we have

$$|\mathsf{Q}_{i-1}^n| \le \frac{4\mathcal{A}_p(nk)^{1-\alpha}(1+h)}{\bar{\delta}\Gamma(2-\alpha)}\max\{|\mathsf{R}_i^n|, |\mathsf{W}_i^n|\}, \tag{4.3}$$

Also, let $\bar{\mathsf{T}} = \max_i\{|\mathsf{T}_i|\}$. From (3.4) and (4.3), we have

$$|\mathsf{q}_{i-1}| \le \frac{4\mathcal{A}_p(nk)^{1-\alpha}(1+h)}{\bar{\delta}\Gamma(2-\alpha)}\max\{|\mathsf{R}_i^0|, |\mathsf{W}_i^0|\} + M_f + \bar{\mathsf{T}}. \tag{4.4}$$

Also, let

$$\gamma_1 = \max\Big\{1, \frac{4\mathcal{A}_p(nk)^{1-\alpha}}{\bar{\delta}\Gamma(2-\alpha)}\Big\}, \qquad \gamma_2 = \{1, h\}.$$

From (4.1)-(4.4), we obtain

$$\max\{|\mathsf{R}_{i-1}|, |\mathsf{W}_{i-1}|, |\mathsf{Q}_{i-1}|, |\mathsf{q}_{i-1}|\} \le (\gamma_1 + h\gamma_1)\max\{|\mathsf{R}_i|, |\mathsf{W}_i|, |\mathsf{Q}_i|, |\mathsf{q}_i|\} + \gamma_2 M_f + \bar{\mathsf{T}}.$$

Iterating this inequality $M$ times, we have

$$\max\{|\mathsf{R}_0|, |\mathsf{W}_0|, |\mathsf{Q}_0|, |\mathsf{q}_0|\} \le (\gamma_1 + h\gamma_1)^M \max\{|\mathsf{R}_M|, |\mathsf{W}_M|, |\mathsf{Q}_M|, |\mathsf{q}_M|\} + \tau(\gamma_2 M_f + \bar{\mathsf{T}}),$$

where $\tau = \sum_{i=0}^{M-1}(\gamma_1 + h\gamma_1)^i$. This inequality implies

$$\max\{|\mathsf{R}_0|, |\mathsf{W}_0|, |\mathsf{Q}_0|, |\mathsf{q}_0|\} \le \gamma_1^M \exp(1)\max\{|\mathsf{R}_M|, |\mathsf{W}_M|, |\mathsf{Q}_M|, |\mathsf{q}_M|\} + \tau(\gamma_2 M_f + \bar{\mathsf{T}}).$$

Letting $\theta_1 = \gamma_1^M \exp(1)$ and $\theta_2 = \tau(\gamma_2 M_f + \bar{\mathsf{T}})$ complete the proof of stability. □

**Theorem 4.2.** *For the marching schemes, when $\varepsilon$, $h$ and $k$ tend towards 0, by choosing $\hat{\delta} = \hat{\delta}(\varepsilon)$, the discrete mollified solution converges to the mollified exact solution.*

**Proof .** First, we define the discrete error functions

$$\Delta\mathsf{R}_i^n = \mathsf{R}_i^n - \upsilon(ih, nk), \quad \Delta\mathsf{W}_i^n = \mathsf{W}_i^n - \upsilon_x(ih, nk), \quad \Delta\mathsf{q}_i = \mathsf{q}_i - q(ih),$$

where $i \in \{0, 1, ..., M\}$ and $n \in \{0, 1, ..., N\}$. By applying Eq. (30) in [4] and theorem (4.6) in [18], we have

$$\begin{aligned}
&|\mathsf{Q}_i^n - \mathrm{D}_{0,t}^\alpha \upsilon(ih, nk)| = |\mathrm{D}_{0,t}^\alpha \mathcal{J}_\delta u^\varepsilon(ih, nk) - \mathrm{D}_{0,t}^\alpha \mathcal{J}_\delta u(ih, nk) + O(k)| \\
&= |\mathrm{D}_{0,t}^\alpha(\mathcal{J}_\delta u^\varepsilon(ih, nk) - \mathcal{J}_\delta u(ih, nk)) + O(k)| \le \frac{1}{\Gamma(1-\alpha)}\int_0^{nk}\frac{4\mathcal{A}_p\varepsilon}{\delta(nk-s)^\alpha}ds + O(k) \\
&= \frac{4\mathcal{A}_p\varepsilon(nk)^{1-\alpha}}{\delta\Gamma(2-\alpha)} + O(k) \le \frac{4\mathcal{A}_p\varepsilon}{\delta\Gamma(2-\alpha)} + O(k) = C_\alpha\frac{\varepsilon}{\delta} + O(k),
\end{aligned} \tag{4.5}$$

where $C_\alpha = \dfrac{4\mathcal{A}_p}{\Gamma(2-\alpha)}$. Expanding the mollified solution $\upsilon(x,t)$ by the Taylor series, we obtain

$$\upsilon((i-1)h,nk) = \upsilon(ih,nk) - h\upsilon_x(ih,nk) + O(h^2), \tag{4.6}$$

$$\upsilon_x((i-1)h,nk) = \upsilon_x(ih,nk) - h(\mathrm{D}^\alpha_{0,t}\upsilon(ih,nk) + q(ih)\upsilon(ih,nk) - f(ih,nk)) + O(h^2), \tag{4.7}$$

$$q((i-1)h) = \frac{1}{\upsilon((i-1)h,0)}(\upsilon_{xx}((i-1)h,0) - \mathrm{D}^\alpha_{0,t}\upsilon((i-1)h,0) + f((i-1)h,0)) + O(h^2). \tag{4.8}$$

From (3.1) and (4.6), we have

$$\begin{aligned}
\Delta\mathsf{R}^n_{i-1} &= \mathsf{R}^n_{i-1} - \upsilon((i-1)h,nk)\\
&= \mathsf{R}^n_i - h\mathsf{W}^n_i - \upsilon((i-1)h,nk)\\
&= \mathsf{R}^n_i - h\mathsf{W}^n_i - \upsilon(ih,nk) + h\upsilon_x(ih,nk) + O(h^2)\\
&= (\mathsf{R}^n_i - \upsilon(ih,nk)) - h(\mathsf{W}^n_i - \upsilon_x(ih,nk)) + O(h^2)\\
&= \Delta\mathsf{R}^n_i - h\Delta\mathsf{W}^n_i + O(h^2).
\end{aligned}$$

and

$$|\Delta\mathsf{R}^n_{i-1}| \le |\Delta\mathsf{R}^n_i| + h|\Delta\mathsf{W}^n_i| + O(h^2). \tag{4.9}$$

By using (3.2), (4.5) and (4.7), we have

$$\begin{aligned}
\Delta\mathsf{W}^n_{i-1} &= \mathsf{W}^n_{i-1} - \upsilon_x((i-1)h,nk)\\
&= \mathsf{W}^n_i - h(\mathsf{Q}^n_i + \mathsf{q}_i\mathsf{R}^n_i - \mathsf{F}^n_i) - \upsilon_x((i-1)h,nk)\\
&= \mathsf{W}^n_i - h(\mathsf{Q}^n_i + \mathsf{q}_i\mathsf{R}^n_i - \mathsf{F}^n_i) - \upsilon_x(ih,nk)\\
&+ h(\mathrm{D}^\alpha_{0,t}\upsilon(ih,nk) + q(ih)\upsilon(ih,nk) - f(ih,nk)) + O(h^2)\\
&= \Delta\mathsf{W}^n_i - h(\Theta_1+\Theta_2) - hC_\alpha\frac{\varepsilon}{\delta} + O(hk) + O(h^2),
\end{aligned}$$

where

$$\Theta_1 = \mathsf{R}^n_i\Delta\mathsf{q}_i, \quad \Theta_2 = q(ih)\Delta\mathsf{R}^n_i.$$

Now, by applying theorem 4.1, we have

$$|\Delta\mathsf{W}^n_{i-1}| \le |\Delta\mathsf{W}^n_i| + hc_1|\Delta\mathsf{R}^n_i| + hc_2|\Delta\mathsf{q}_i| + hC_\alpha\frac{\varepsilon}{\delta} + O(hk) + O(h^2). \tag{4.10}$$

From (3.4) and (4.8), we obtain

$$\begin{aligned}
\Delta\mathsf{q}_{i-1} &= \mathsf{q}_{i-1} - q((i-1)h)\\
&= \frac{1}{\mathsf{R}^0_{i-1}}(\mathsf{T}_{i-1} - \mathsf{Q}^0_{i-1} + \mathsf{F}^0_{i-1}) - q((i-1)h)\\
&= \frac{1}{\mathsf{R}^0_{i-1}}(\mathsf{T}_{i-1} - \mathsf{Q}^0_{i-1} + \mathsf{F}^0_{i-1}) - \frac{1}{\upsilon((i-1)h,0)}\Big(\upsilon_{xx}((i-1)h,0)\\
&- \mathrm{D}^\alpha_{0,t}\upsilon((i-1)h,0) + f((i-1)h,0)\Big) + O(h^2)\\
&= \Phi_1 - \Phi_2 + \Phi_3 f((i-1)h,0) + O(h^2),
\end{aligned}$$

where

$$\Phi_1 = \frac{\mathsf{T}_{i-1}}{\mathsf{R}^0_{i-1}} - \frac{\mathfrak{D}^2(\upsilon((i-1)h,0))}{\upsilon((i-1)h,0)},$$

$$\Phi_2 = \frac{\mathsf{Q}^0_{i-1}}{\mathsf{R}^0_{i-1}} - \frac{\mathrm{D}^{\alpha}_{0,t} v((i-1)h,0)}{v((i-1)h,0)},$$
$$\Phi_3 = \frac{1}{\mathsf{R}^0_{i-1}} - \frac{1}{v((i-1)h,0)}.$$

Notice that

$$\Phi_1 = \mathfrak{D}^2(v((i-1)h,0))\Phi_3 + \frac{1}{\mathsf{R}^0_{i-1}}\Delta\mathsf{T}_{i-1}, \tag{4.11}$$

in which $\Delta\mathsf{T}_i = \mathsf{T}_i - \mathfrak{D}^2(v(ih,0))$ and

$$\Phi_2 = \mathrm{D}^{\alpha}_{0,t} v((i-1)h,0)\Phi_3 + \frac{1}{\mathsf{R}^0_{i-1}}\Delta\mathsf{Q}^0_{i-1}. \tag{4.12}$$

Let $M_t = \max_i\{|\mathsf{T}_i|\}$, $m_0 = \min_i\{|\mathsf{R}^0_i|\}$. By applying theorem (4.8) in [18], we have

$$|\Delta\mathsf{T}_i| = |\mathsf{T}_i - \mathfrak{D}^2(v(ih,0))| \leq \bar{C}_1\frac{\varepsilon}{\delta'}. \tag{4.13}$$

Now by using (4.11) and (4.13), we obtain

$$\begin{aligned} |\Phi_1| &\leq |\mathfrak{D}^2(v((i-1)h,0))||\Phi_3| + \frac{1}{|\mathsf{R}^0_{i-1}|}|\Delta\mathsf{T}_{i-1}| \\ &\leq M_t|\Phi_3| + \frac{\bar{C}_1\varepsilon}{\delta' m_0}. \end{aligned}$$

Also let $M_0 = \max_i\{|\mathsf{R}^0_i|\}$, by using Eq.(30) in [4], (4.5) and (4.12), we have

$$\begin{aligned} |\Phi_2| &\leq |\mathrm{D}^{\alpha}_{0,t} v((i-1)h,0)||\Phi_3| + \frac{1}{|\mathsf{R}^0_{i-1}|}|\Delta\mathsf{Q}^0_{i-1}| \\ &\leq \frac{4\mathcal{A}_p M_0}{\delta'\Gamma(2-\alpha)}|\Phi_3| + \frac{1}{m_0}\Big(C_\alpha\frac{\varepsilon}{\delta'} + O(k)\Big), \end{aligned}$$

and by applying theorem (4.2) in [18], we have

$$|\Phi_3| \leq \frac{C}{m_0^2}(\delta' + h).$$

Thus, we have

$$|\Phi_1| \leq \frac{M_t}{m_0^2}C(\delta' + h) + \frac{\bar{C}_1\varepsilon}{\delta' m_0},$$
$$|\Phi_2| \leq \frac{4\mathcal{A}_p C M_0}{\delta'\Gamma(2-\alpha)m_0^2}(\delta' + h) + \frac{1}{m_0}\Big(C_\alpha\frac{\varepsilon}{\delta'} + O(k)\Big).$$

Let $\hat{M}_f = \max_{i,j}\{|f(ih,jk))|\}$. Hence, we obtain

$$\begin{aligned} |\Delta\mathsf{q}_{i-1}| &\leq |\Phi_1| + |\Phi_2| + |\Phi_3||f((i-1)h,0)| + O(h^2) \\ &\leq \Psi_1 + \Psi_2 + O(h^2), \end{aligned} \tag{4.14}$$

where

$$\Psi_1 = \frac{C}{m_0^2}\Big(M_t + \frac{4\mathcal{A}_p M_0}{\delta'\Gamma(2-\alpha)} + \hat{M}_f\Big)(\delta' + h), \quad \Psi_2 = \frac{1}{m_0}\Big(\bar{C}_1\frac{\varepsilon}{\delta'} + C_\alpha\frac{\varepsilon}{\delta'} + O(k)\Big).$$

Let $|\Delta \mathsf{R_i}| = \max\limits_{0\le n\le N} |\Delta \mathsf{R}_i^n|$, $|\Delta \mathsf{W}_i| = \max\limits_{0\le n\le N} |\Delta \mathsf{W}_i^n|$ and $\hat{\theta} = hC_\alpha \dfrac{\varepsilon}{\delta} + O(hk) + O(h^2)$.
Thus, from (4.9), (4.10), we obtain

$$\begin{aligned} |\Delta \mathsf{R}_{i-1}| &\le |\Delta \mathsf{R}_i| + h|\Delta \mathsf{W}_i| + O(h^2), \\ |\Delta \mathsf{W}_{i-1}| &\le |\Delta \mathsf{W}_i| + hc_1|\Delta \mathsf{R}_i| + hc_2|\Delta \mathsf{q}_i| + \hat{\theta}, \end{aligned}$$

hence

$$\begin{aligned} |\Delta \mathsf{R}_{i-1}| &\le (1+h)\max\{|\Delta \mathsf{R}_i|, |\Delta \mathsf{W}_i|\} + O(h^2), \\ |\Delta \mathsf{W}_{i-1}| &\le (1+hc_1)\max\{|\Delta \mathsf{R}_i|, |\Delta \mathsf{W}_i|\} + hc_2(\Psi_1 + \Psi_2 + O(h^2)) + \hat{\theta}. \end{aligned}$$

Let $\lambda = \max\{1, c_1\}$. Then, we have

$$\max\{|\Delta \mathsf{R}_{i-1}|, |\Delta \mathsf{W}_{i-1}|\} \le (1+\lambda h)\max\{|\Delta \mathsf{R}_i|, |\Delta \mathsf{W}_i|\} + \Lambda,$$

where $\Lambda = hc_2(\Psi_1 + \Psi_2 + O(h^2)) + O(h^2) + \hat{\theta}$. Now let $\Delta_i = \max\{|\Delta \mathsf{R}_i|, |\Delta \mathsf{W}_i|\}$. Thus, we have

$$\Delta_{i-1} \le (1+\lambda h)\Delta_i + \Lambda, \tag{4.15}$$

and

$$\Delta_0 \le (1+\lambda h)\Delta_1 + \Lambda \le (1+\lambda h)^2\Delta_2 + (1+\lambda h)\Lambda + \Lambda \le ... \le (1+\lambda h)^M \Delta_M + \tau\Lambda, \tag{4.16}$$

where $\tau = \sum\limits_{i=0}^{M-1} (\lambda_1 + h\lambda_2)^i$. Now by using theorem (4.2) in [18], for $n \in \{0, 1, ..., N\}$, there exists constant $C_n$ and $D_n$, such that

$$\begin{aligned} |\Delta \mathsf{R}_M^n| &= |\mathsf{R}_M^n - v(1, nk)| \le C_n(\delta + k), \\ |\Delta \mathsf{W}_M^n| &= |\mathsf{W}_M^n - v_x(1, nk)| \le D_n(\delta + k). \end{aligned}$$

Let $C' = \max\{C_n, D_n|\ n = 0, ..., N\}$, then we have

$$\Delta_M = \max\{|\Delta \mathsf{R}_M^n|, |\Delta \mathsf{W}_M^n|\} \le C'(\delta + k),$$

and

$$\Delta_0 \le exp(\lambda)C'(\delta + k) + \tau\Lambda. \tag{4.17}$$

As a result, when $\varepsilon$, $h$ and $k$ tend towards 0, by choosing $\hat{\delta} = \hat{\delta}(\varepsilon)$, $\delta$ and $\Lambda$ tend towards 0. Thus, $\Delta_0$ will tend to 0. It completes the proof. □

## 5. Numerical examples for reconstruction of the unknown reaction coefficient

In this section, two examples are solved to test the ability of the proposed algorithm.
To simulate the data for the inverse problem, some random noises are added to the data resulted from the additional functions. Suppose that $\varepsilon$ indicates a relative noise level in the data. Then, for generating noisy data, we use the formula

$$s^\varepsilon(t_i) = s(t_i)(1 + \varepsilon \times rand(i)),$$

where $rand(i)$ is a random number uniformly distributed in $[-1, 1]$. Also, to demonstrate the accuracy of our method, by using the $L^2$-norm

$$E_{L_2}(h, k) = \max_{1\le n\le N} \|u^n - U^n\|,$$

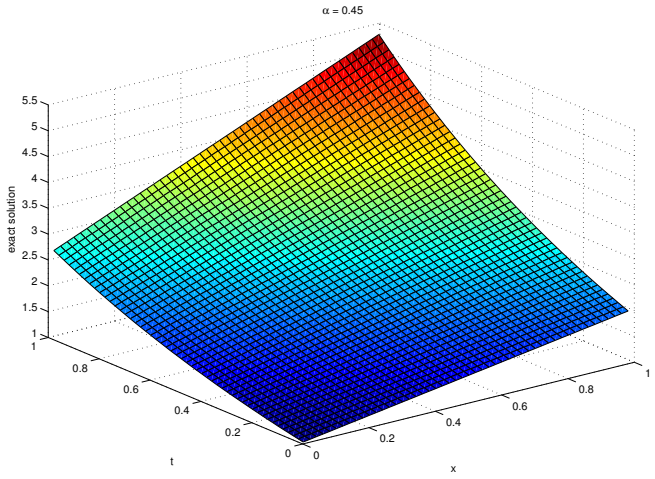


Figure 2: The exact solution of Example 5.1 when $\alpha = 0.45$.

we calculate the convergence order of proposed method with the following formulas

$$Order(h) = \log_{\frac{h1}{h2}} \Big(\frac{E_{L_2}(h_1, k)}{E_{L_2}(h_2, k)}\Big), \qquad Order(k) = \log_{\frac{k1}{k2}} \Big(\frac{E_{L_2}(h, k_1)}{E_{L_2}(h, k_2)}\Big).$$

The computations are performed on a personal computer using a 2.20 GHz processor and the codes are written in Matlab $R2014a$.

**Example 5.1.** *In this example, we work on the test problem presented in Section 2. The exact solution of this problem is*

$$u(x,t) = e^x(1+t),$$

*and* $q(x) = E_\alpha(x^\alpha)(1-x)$.

Figure 2 shows the exact solutions and Figure 3, Figure 4 and Figure 5 show the numerical solutions and absolute error of $u(x,t)$ when $\alpha = 0.45, M = 150, N = 150$ and $\varepsilon = 1\%, 5\%, 10\%$. Figure 6 shows the comparison between the exact and the computed solutions of $q(x)$ with regularization and without regularization when $\alpha = 0.45$, $M = 100$, $N = 150$ and $\varepsilon = 5\%$. Figure 7 displays the behaviour of numerical approximations to $q(x)$ when $\alpha = 0.25$, $M = 100$, and $N = 150$ for various noise levels.
Furthermore, Figure 8 shows the exact and the estimated solutions to $q(x)$ for several values of $\alpha$ when $M = 100$, $N = 150$ and $\varepsilon = 1\%$.
Finally, let $h = 1/100$. Taking different time steps, Table 1 presents the maximum $L_2$-norm errors and convergence orders of the method. Again, fixing the temporal step $k = 1/150$ and taking different spatial steps, Table 2 presents the $L_2$-norm errors and convergence orders in spatial direction.

**Example 5.2.** *Consider Eq. (1.1) with*

$$f(x,t) = \frac{\Gamma(3)}{\Gamma(3-\alpha)} t^{2-\alpha} x^2 + 2\sin(4\pi x)(x^2(1+t^2) - x + e^{x-1}) - 2t^2 - e^{x-1} - 2.$$

*Also, let* $u_0(x) = x^2 - x + e^{x-1}$, $\sigma = 1 - e$, $\gamma = -2$ *and* $\phi(t) = 1 + t^2$. *The exact solution of this problem is* $u(x,t) = e^{x-1} - x + x^2(1+t^2)$ *and* $q(x) = 2\sin(4\pi x)$.

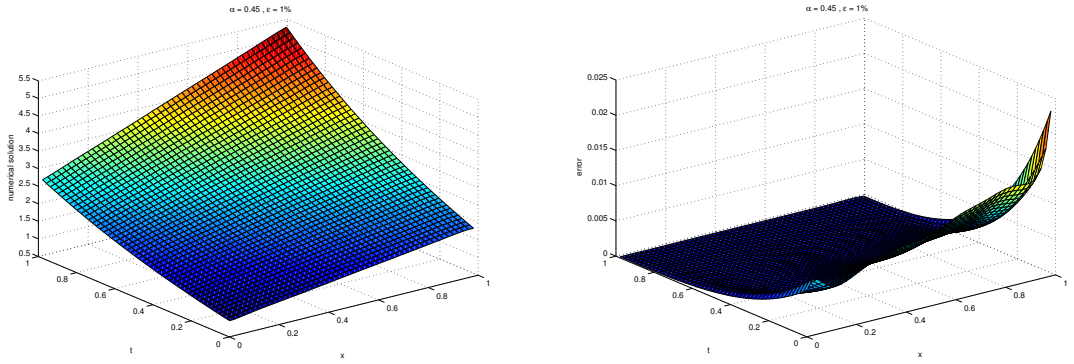


Figure 3: The numerical solution and its absolute error for Example 5.1 when $\alpha = 0.45$ and $\varepsilon = 1\%$.

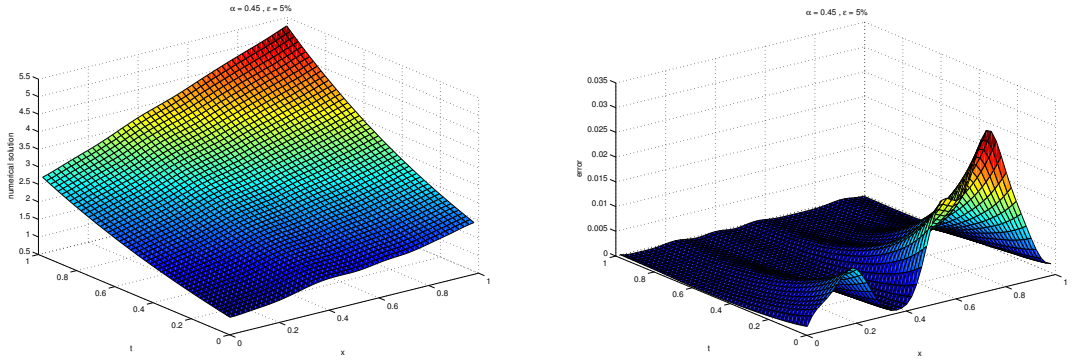


Figure 4: The numerical solutions and its absolute error for Example 5.1 when $\alpha = 0.45$ and $\varepsilon = 5\%$.

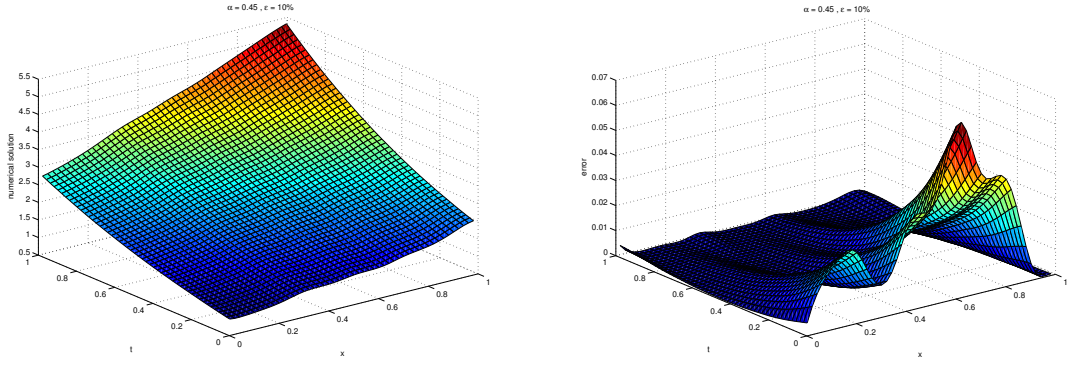


Figure 5: The numerical solutions and its absolute error for Example 5.1 when $\alpha = 0.45$ and $\varepsilon = 10\%$.

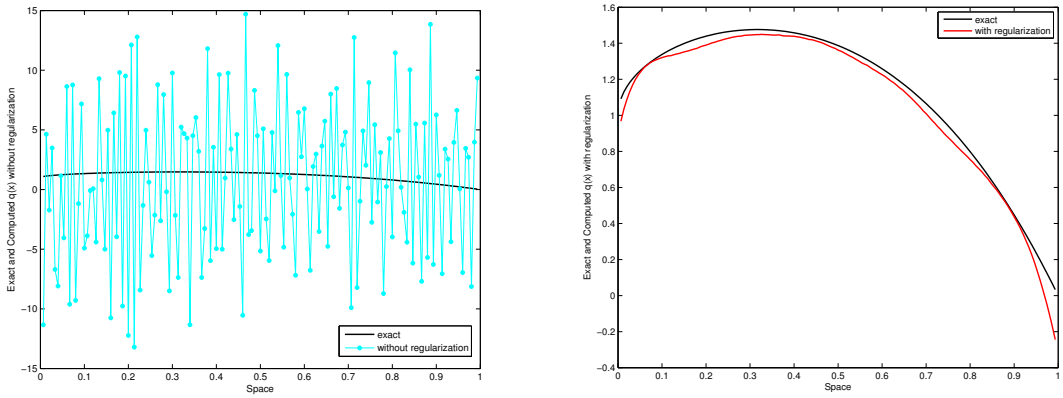


Figure 6: The exact and numerical values of $q(x)$ in Example 5.1 when $\alpha = 0.45$ and $\varepsilon = 5\%$. Left: without regularization. Right: with regularization.

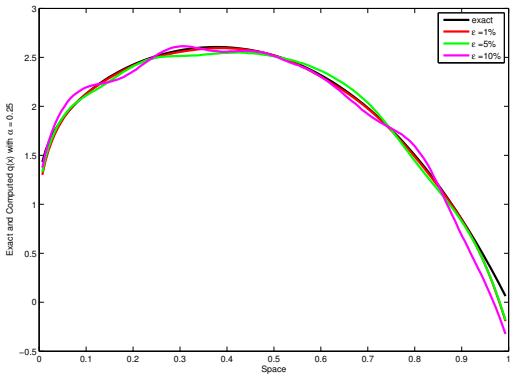


Figure 7: The numerical approximations to $q(x)$ in Example 5.1 for several noise levels when $\alpha = 0.25$.

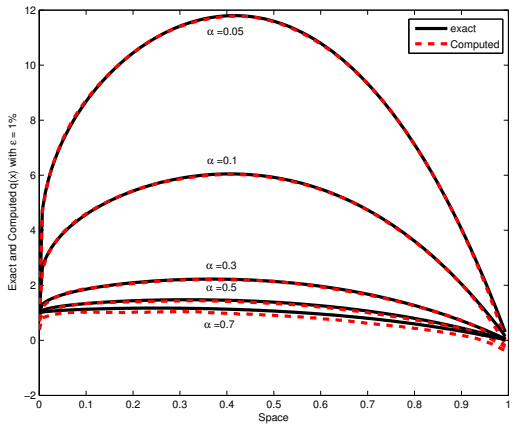


Figure 8: The exact and numerical approximations to $q(x)$ in Example 5.1 for various values of $\alpha$ when $\varepsilon = 1\%$ .

Table 1: The maximum $L_2$-norm errors and convergence orders for Example 5.1 when $h = 1/100$.

| $\alpha$ | $k$ | $E_{L_2}$ | $Order(k)$ | $E_{L_2}$ | $Order(k)$ | $E_{L_2}$ | $Order(k)$ |
|---|---|---|---|---|---|---|---|
| | | $\varepsilon = 1\%$ | | $\varepsilon = 5\%$ | | $\varepsilon = 10\%$ | |
| 0.25 | 1/25 | 0.2606 | $*$ | 0.4667 | $*$ | 0.7089 | $*$ |
| | 1/50 | 0.1022 | 1.3504 | 0.1884 | 1.3087 | 0.2891 | 1.2940 |
| | 1/100 | 0.0355 | 1.6092 | 0.0652 | 1.5309 | 0.1035 | 1.4819 |
| | 1/200 | 0.0092 | 1.8645 | 0.0185 | 1.8173 | 0.0306 | 1.7580 |
| 0.5 | 1/25 | 0.3340 | $*$ | 0.6045 | $*$ | 0.8561 | $*$ |
| | 1/50 | 0.1221 | 1.4518 | 0.2287 | 1.4023 | 0.3285 | 1.3819 |
| | 1/100 | 0.0400 | 1.6100 | 0.0771 | 1.5687 | 0.1152 | 1.5118 |
| | 1/200 | 0.0107 | 1.9024 | 0.0215 | 1.8424 | 0.0329 | 1.8080 |
| 0.75 | 1/25 | 0.4522 | $*$ | 0.8002 | $*$ | 0.9901 | $*$ |
| | 1/50 | 0.1486 | 1.6055 | 0.2712 | 1.5610 | 0.3640 | 1.4436 |
| | 1/100 | 0.0425 | 1.8059 | 0.0825 | 1.7169 | 0.1200 | 1.6009 |
| | 1/200 | 0.0110 | 1.9500 | 0.0221 | 1.9003 | 0.0332 | 1.8538 |

Table 2: The maximum $L_2$-norm errors and convergence orders for Example 5.1 when $k = 1/150$.

| $\alpha$ | $h$ | $E_{L_2}$ | $Order(h)$ | $E_{L_2}$ | $Order(h)$ | $E_{L_2}$ | $Order(h)$ |
|---|---|---|---|---|---|---|---|
| | | $\varepsilon = 1\%$ | | $\varepsilon = 5\%$ | | $\varepsilon = 10\%$ | |
| 0.25 | 1/25 | 0.0955 | $*$ | 0.1746 | $*$ | 0.3081 | $*$ |
| | 1/50 | 0.0446 | 1.0985 | 0.0751 | 1.2172 | 0.1406 | 1.1318 |
| | 1/100 | 0.0191 | 1.2235 | 0.0310 | 1.2765 | 0.0610 | 1.2047 |
| | 1/200 | 0.0076 | 1.3295 | 0.0121 | 1.3573 | 0.0223 | 1.4518 |
| 0.5 | 1/25 | 0.1224 | $*$ | 0.2508 | $*$ | 0.4990 | $*$ |
| | 1/50 | 0.0554 | 1.1436 | 0.1111 | 1.1747 | 0.2121 | 1.2343 |
| | 1/100 | 0.0240 | 1.2069 | 0.0436 | 1.3495 | 0.0803 | 1.4013 |
| | 1/200 | 0.0094 | 1.3523 | 0.0163 | 1.4195 | 0.0261 | 1.6214 |
| 0.75 | 1/25 | 0.1936 | $*$ | 0.4011 | $*$ | 0.6432 | $*$ |
| | 1/50 | 0.0813 | 1.2518 | 0.1725 | 1.2174 | 0.2521 | 1.3513 |
| | 1/100 | 0.0304 | 1.4192 | 0.0634 | 1.4440 | 0.0901 | 1.4844 |
| | 1/200 | 0.0106 | 1.5200 | 0.0208 | 1.6079 | 0.0280 | 1.6861 |

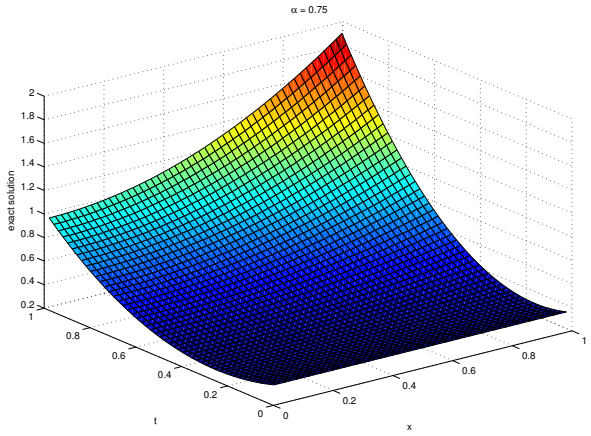


Figure 9: The exact solution of Example 5.2 when $\alpha = 0.75$.

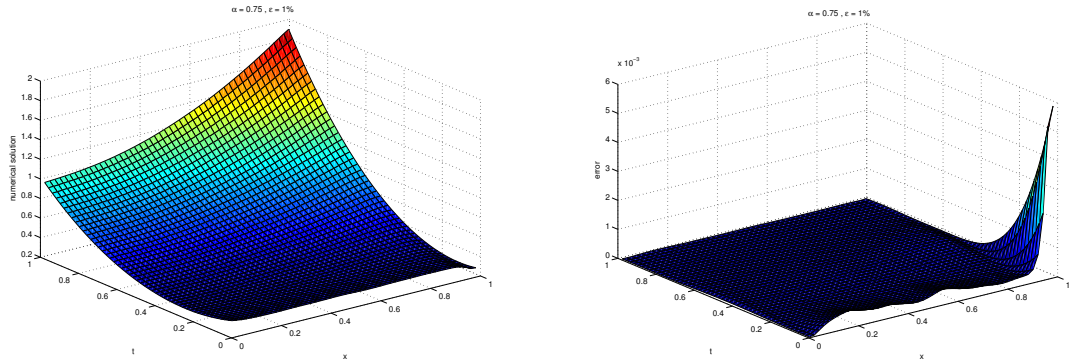


Figure 10: The numerical solution and its absolute error for Example 5.2 when $\alpha = 0.75$ and $\varepsilon = 1\%$.

Figure 9 shows the exact solutions and Figure 10, Figure 11 and Figure 12 show the numerical solutions and absolute error of $u(x,t)$ when $\alpha = 0.75, M = 150, N = 150$ and $\varepsilon = 1\%, 5\%, 10\%$. Figure 13 shows the comparison between the exact and the computed solutions of $q(x)$ with regularization and without regularization when $\alpha = 0.5$, $M = 100$, $N = 150$ and $\varepsilon = 5\%$. Let $h = 1/100$. Taking different time steps, Table 3 presents the maximum $L_2$-norm errors and convergence orders of the method. Again, fixing the temporal step $k = 1/150$ and taking different spatial steps, Table 4 presents the $L_2$-norm errors and convergence orders in spatial direction. Figure 14 displays the behaviour of numerical approximations to $q(x)$ when $\alpha = 0.3$, $M = 150$, and $N = 200$ for various noise levels.

## 6. Conclusion

In this paper, the inverse problem of recovering the reaction coefficient for the time-fractional reaction-diffusion equation under the Robin boundary conditions was investigated. The mollification regularization method was applied to regularize the problem and a marching finite difference scheme was used to find the numerical solution. The stability of the algorithm and its convergence were verified and some test problems were solved. To simulate the data for the inverse problem some random errors were added to the exact data functions. The recovered reaction coefficient and the

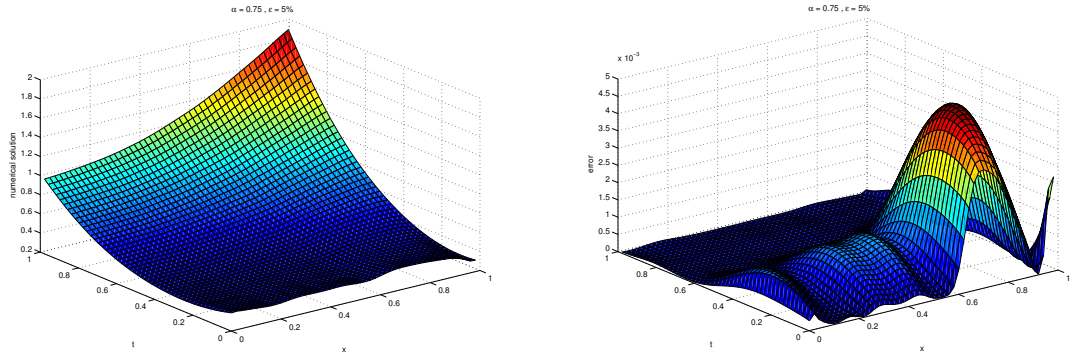


Figure 11: The numerical solution and its absolute error for Example 5.2 when $\alpha = 0.75$ and $\varepsilon = 5\%$.

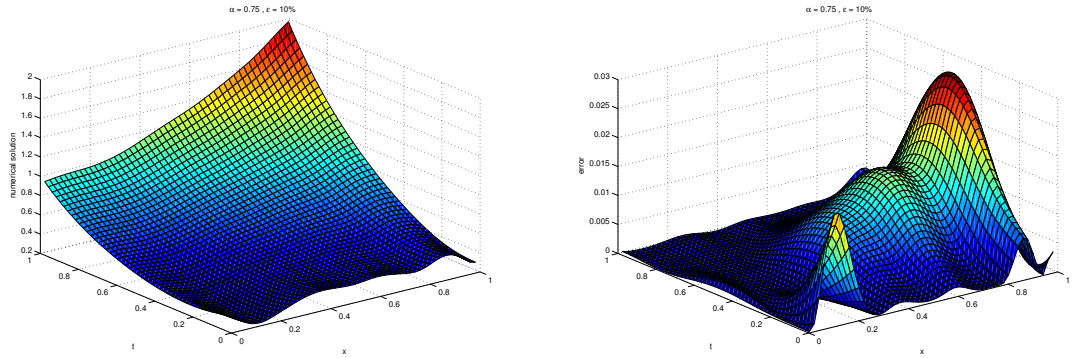


Figure 12: The numerical solution and its absolute error for Example 5.2 when $\alpha = 0.75$ and $\varepsilon = 10\%$.

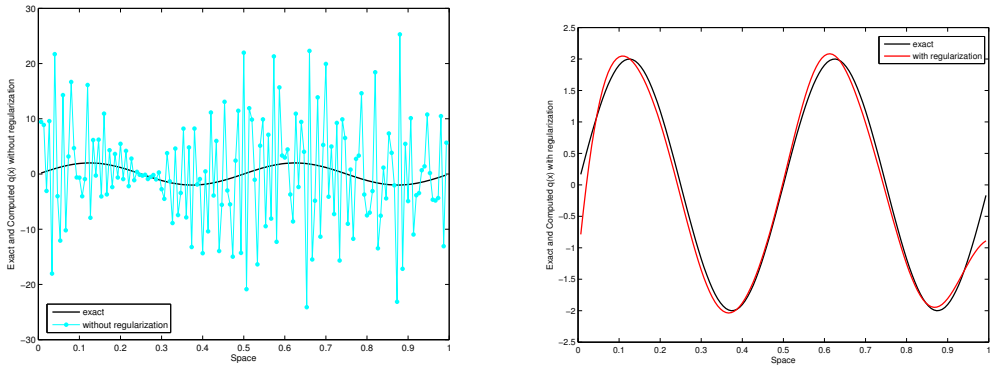


Figure 13: The exact and numerical values of $q(x)$ in Example 5.2 when $\alpha = 0.5$ and $\varepsilon = 5\%$. Left: without regularization. Right: with regularization.

Table 3: The maximum $L_2$-norm errors and convergence orders for Example 5.2 when $h = 1/100$.

| $\alpha$ | $k$ | $E_{L_2}$ | $Order(k)$ | $E_{L_2}$ | $Order(k)$ | $E_{L_2}$ | $Order(k)$ |
|---|---|---|---|---|---|---|---|
| | | $\varepsilon = 1\%$ | | $\varepsilon = 5\%$ | | $\varepsilon = 10\%$ | |
| 0.25 | 1/25 | 0.0643 | $*$ | 0.1777 | $*$ | 0.2785 | $*$ |
| | 1/50 | 0.0296 | 1.1192 | 0.0801 | 1.1496 | 0.1211 | 1.2015 |
| | 1/100 | 0.0131 | 1.1760 | 0.0352 | 1.1862 | 0.0506 | 1.2590 |
| | 1/200 | 0.0057 | 1.2005 | 0.0146 | 1.2696 | 0.0194 | 1.3831 |
| 0.5 | 1/25 | 0.0737 | $*$ | 0.1945 | $*$ | 0.3483 | $*$ |
| | 1/50 | 0.0322 | 1.1946 | 0.0866 | 1.1673 | 0.1497 | 1.2183 |
| | 1/100 | 0.0140 | 1.2016 | 0.0372 | 1.2191 | 0.0602 | 1.3142 |
| | 1/200 | 0.0060 | 1.2224 | 0.0151 | 1.3008 | 0.0229 | 1.3944 |
| 0.75 | 1/25 | 0.0981 | $*$ | 0.2219 | $*$ | 0.4150 | $*$ |
| | 1/50 | 0.0424 | 1.2102 | 0.0949 | 1.2254 | 0.1731 | 1.2615 |
| | 1/100 | 0.0178 | 1.2522 | 0.0380 | 1.3204 | 0.0686 | 1.3353 |
| | 1/200 | 0.0071 | 1.3260 | 0.0141 | 1.4303 | 0.0244 | 1.4913 |

Table 4: The maximum $L_2$-norm errors and convergence orders for Example 5.2 when $k = 1/150$.

| $\alpha$ | $h$ | $E_{L_2}$ | $Order(h)$ | $E_{L_2}$ | $Order(h)$ | $E_{L_2}$ | $Order(h)$ |
|---|---|---|---|---|---|---|---|
| | | $\varepsilon = 1\%$ | | $\varepsilon = 5\%$ | | $\varepsilon = 10\%$ | |
| 0.25 | 1/25 | 0.0244 | $*$ | 0.0523 | $*$ | 0.0917 | $*$ |
| | 1/50 | 0.0130 | 0.9084 | 0.0258 | 1.0194 | 0.0420 | 1.1265 |
| | 1/100 | 0.0064 | 1.0224 | 0.0116 | 1.1532 | 0.0186 | 1.1751 |
| | 1/200 | 0.0028 | 1.1926 | 0.0050 | 1.2141 | 0.0078 | 1.2538 |
| 0.5 | 1/25 | 0.0327 | $*$ | 0.0680 | $*$ | 0.1067 | $*$ |
| | 1/50 | 0.0162 | 1.0133 | 0.0309 | 1.1379 | 0.0462 | 1.2076 |
| | 1/100 | 0.0075 | 1.1110 | 0.0137 | 1.1734 | 0.0194 | 1.2518 |
| | 1/200 | 0.0032 | 1.2288 | 0.0058 | 1.2401 | 0.0080 | 1.2780 |
| 0.75 | 1/25 | 0.0493 | $*$ | 0.0812 | $*$ | 0.1228 | $*$ |
| | 1/50 | 0.0227 | 1.1187 | 0.0356 | 1.1896 | 0.0527 | 1.2204 |
| | 1/100 | 0.0101 | 1.1683 | 0.0148 | 1.2663 | 0.0216 | 1.2868 |
| | 1/200 | 0.0043 | 1.2319 | 0.0061 | 1.2787 | 0.0087 | 1.3119 |

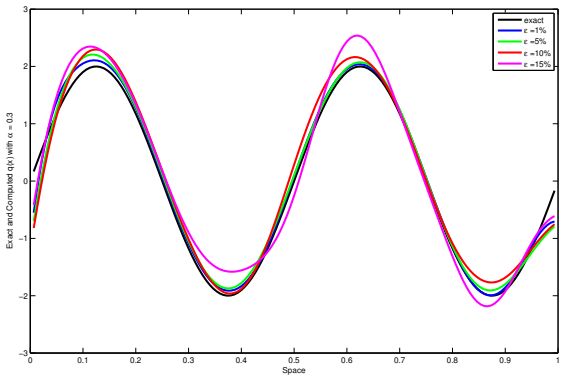


Figure 14: The numerical approximations to $q(x)$ in Example 5.2 for several noise levels when $\alpha = 0.3$.

approximated solution of the fractional reaction-diffusion equation were displayed in some suitable graphs. Furthermore, the maximum $L^2$-norm errors and convergence orders of the method for different values of $h$ and $k$ were presented in some tables. The proposed numerical scheme is fast and convenient in implementation. The numerical results verify the high accuracy of the method. The obtained convergence orders are more than one. This confirms that the convergence speed of the method for solving the inverse problem is good, even in the presence of the noise up to ten percent.

## References

[1] A. Aldoghaither, D.Y. Liu and T.M. Laleg-Kirati, *Modulating functions based algorithm for the estimation of the coefficients and differentiation order for a space-fractional advection-dispersion equation*, SIAM J. Sci. Comput. 37 (2015) 2813–2839.

[2] S.R. Arridge and J.C. Schotland, *Optical tomography: forward and inverse problems*, Inverse Probl. 25 (2009) 123010.

[3] A. Babaei and S. Banihashemi, *A stable numerical approach to solve a time-fractional inverse heat conduction problem*, Iran J. Sci. Technol. Trans. Sci. 42 (2018) 2225–2236.

[4] A. Babaei and S. Banihashemi, *Reconstructing unknown nonlinear boundary conditions in a time-fractional inverse reaction–diffusion–convection problem*, Numer. Methods Part. Differ. Equ. 35 (2018) 976–992.

[5] D. Baleanu, J.A. Tenreiro Machado, A.C.J. Luo, *Fractional Dynamics and Control*, Springer, New York, 2012.

[6] J.V. Beck , B. Blackwell and C.R. Clair, *Inverse Heat Conduction: Ill-Posed Problems*, New York, 1985.

[7] A.S. Chaves, *A fractional diffusion equation to describe Levy flights*, Phys. Lett. A 239 (1998) 13–16.

[8] F.F. Dou and Y.C. Hon, *Numerical computation for backward time-fractional diffusion equation*, Eng. Anal. Boundary Elem. 40 (2014) 138–146.

[9] D.N. Ghosh Roy and L.S. Couchman, *Inverse Problems and Inverse Scattering of Plane Waves*, Academic Press, New York, 2002.

[10] R. Gorenflo, F. Mainardi, D. Moretti, G. Pagnini and P. Paradisi, *Fractional diffusion: probability distributions and random walk models*, Phys. A 305 (2002) 106–112.

[11] B.I. Henry and S.L. Wearne, *Fractional reaction–diffusion*, Phys. A 276 (2000) 448–455.

[12] H. Jafari, K. Sayevand, H. Tajadodi and D. Baleanu, *Homotopy analysis method for solving Abel differential equation of fractional order*, Cent. Eur. J. Phys. 11 (2013) 1523–1527.

[13] B. Jin and W. Rundell, *A tutorial on inverse problems for anomalous diffusion processes*, Inverse Probl. 31 (2015) 035003.

[14] B. Jin and W. Rundell, *An inverse problem for a one-dimensional time-fractional diffusion problem*, Inverse Probl. 28 (2012) 075010.

[15] Y. Luchko, W. Rundell, M. Yamamoto and L. Zuo, *Uniqueness and reconstruction of an unknown semilinear term in a time-fractional reaction-diffusion equation*, Inverse Probl. 29 (2013) 065019.

[16] M.M. Meerschaert and C. Tadjeran, *Finite difference approximations for fractional advection-dispersion flow equations*, J. Comput. Appl. Math. 172 (2004) 65–77.
[17] R. Metzler and J. Klafter, *The random walk's guide to anomalous diffusion: A fractional dynamics approach*, Phys. Rep. 339 (2000) 1–77.
[18] D.A. Murio, *Mollification and space marching, in: K. Woodbury (Ed.), Inverse Engineering Handbook*, CRC Press, Boca Raton, FL, (2002).
[19] D.A. Murio, *On the stable numerical evaluation of Caputo fractional derivatives*, Comput. Math. Appl. 51 (2006) 1539–1550.
[20] D.A. Murio, *Time fractional IHCP with Caputo fractional derivatives*, Comput. Math. Appl. 56 (2008) 2371–2381.
[21] K.B. Oldham and J. Spanier, *The Fractional Calculus: Theory and Application of Differentiation and Integration to Arbitrary Order*, Academic Press, New York, 1974.
[22] V. Penenko, A.Baklanov, E. Tsvetova and A. Mahura, *Direct and inverse problems in a variational concept of environmental modeling*, Pure Appl. Geophys. 169 (2012) 447–465.
[23] C.M.A. Pinto, A.R.M. Carvalho, *A latency fractional order model for HIV dynamics*, J. Comput. Appl. Math. 312 (2017) 240–256.
[24] I. Podlubny, *Fractional Differential Equations*, Academic Press, New York, 1999.
[25] M. Prato and L. Zanni, *Inverse problems in machine learning: an application to brain activity interpretation*, J. Phys. Conf. Ser. 135 (2008) 012085.
[26] E. Scalas, R. Gorenflo and F. Mainardi, *Fractional calculus and continuous-time finance*, Phys. A 284 (2000) 376–384.
[27] K. Seki, M. Wojcik and M. Tachiya, *Fractional reaction–diffusion equation*, J. Chem. Phys. 119 (2003) 2165–2174.
[28] X. Song, G. Zheng and L. Jiang, *Recovering the reaction coefficient for two dimensional time fractional diffusion equations*, (2017),- arXiv:1707.00671 [math.NA].
[29] C. Sun, G. Li, and X. Jia, *Simultaneous inversion for the diffusion and source coefficients in the multi-term TFDE*, Inverse Probl. Sci. Eng. 25 (2017) 1–21.
[30] A. Taghavi, A. Babaei, A. Mohammadpour, *A stable numerical scheme for a time fractional inverse parabolic equation*, Inverse Probl. Sci. Eng. 25 (2017) 1474–1491.
[31] D. Trucu, D.B. Ingham and D. Lesnic, *Inverse space-dependent perfusion coefficient identification*, J. Phys. Conf. Ser. 135 (2008) 012098.
[32] V.K. Tuan, *Inverse problem for fractional diffusion equation,* Fract. Calc. Appl. Anal. 14 (2011) 31–55.
[33] V.K. Tuan and N.S. Hoang, *An inverse problem for a multidimensional fractional diffusion equations*, Anal. 36 (2016) 107–122.
[34] N.H. Tuan, L.D. Long, V.T. Nguyen and T. Tran, *On a final value problem for the time-fractional diffusion equation with inhomogeneous source*, Inverse Probl. Sci. Eng. 25 (2017) 1367–1395.
[35] T. Wei and Z.Q. Zhang, *Reconstruction of a time-dependent source term in a time-fractional diffusion equation*, Eng. Anal. Boundary Elem. 37 (2013) 23–31.
[36] L. Yan and F. Yang, *Effcient Kansa-type MFS algorithm for time-fractional inverse diffusion problems*, Comput. Math. Appl. 67 (2014) 1507–1520.
[37] X.J. Yang, *Advanced Local Fractional Calculus and its Applications*, World Science Publisher LLC, New York, USA, 2012.
[38] G.H. Zheng and T. Wei, *Spectral regularization method for the time fractional inverse advection-dispersion equation*, J. Comput. Appl. Math. 233 (2010) 2631–2640.
[39] Y. Zhou, *Basic Theory of Fractional Differential Equations*, World Scientific, Singapore, 2014.